Estimation of Tire Slip Angle and Friction Limits Using Steering Torque

Yung-Hsiang Judy Hsu, Shad M. Laws, and J. Christian Gerdes

***Abstract*—Knowledge of the vehicle's lateral handling limits is important for vehicle control systems which aim to enhance vehicle handling and passenger safety. This paper presents a model-based estimation method that utilizes pneumatic trail information in steering torque to identify a vehicle's lateral handling limits, which are defined by the tire slip angle and peak lateral force limits. This method uses measurements available on many current production vehicles. Most importantly, it takes advantage of the early friction information encoded in the tire pneumatic trail. Pneumatic trail decreases as a function of the tire parameters even in the linear handling region, enabling early detection of the limits *before* they are reached. Experimental results on an independent front steering steer-by-wire research vehicle demonstrate the observer's ability to provide accurate real-time estimates of tire slip angle up to the limits of handling. Testing conditions include maneuvers performed on dry, flat paved road, as well as on lower-friction, dry gravel.**

***Index Terms*—Aligning moment, friction, pneumatic trail, sideslip, slip angle, steering torque, tire properties.**

I. Introduction

WORLDWIDE, an estimated 1.2 million people are killed in road crashes each year and as many as 50 million are injured. Projections indicate that these figures may increase by about 65% over the next 20 years unless there is new commitment to prevention [1]. Over the past few decades, vehicle control systems have been developed to enhance vehicle handling and passenger safety. These systems seek to prevent unintended vehicle behavior through active vehicle control and assist drivers in maintaining control of their vehicles. Some notable examples include anti-lock brake systems (ABS), traction control, and electronic stability control (ESC) systems.

While current vehicle safety systems are unquestionably life-saving technologies, they unfortunately are limited by the lack of knowledge of the vehicle's state and operating conditions. Knowledge of the vehicle's sideslip angle, which relates its lateral velocity to its longitudinal velocity, is largely unavailable for current safety systems; systems such as ESC have access to measurements of sideslip rate, not sideslip angle. Approaches that determine sideslip angle from sideslip rate integration are often prone to uncertainty and errors from sensor biases, road grade and bank angle [2]. Methods that design observers to estimate sideslip often depend on accurate tire parametrization, which is problematic since tire parameters vary based on the road surface [3]–[5]. Information about the tires' lateral handling limits, which are determined by the available tire-road friction and normal force, is also unavailable to current systems.

As a result of this limited information, production stability control systems rely on detecting a difference between intended and actual vehicle yaw rate before the system can intervene [6], [7]. In other words, current systems are reactive; they must detect a problem before corrective action can be taken. If onboard systems had accurate knowledge of sideslip angle (and therefore tire slip angle) and could predict the peak lateral force limits, control systems could anticipate rather than react to loss of control situations, further enhancing vehicle handling and increasing passenger safety [7].

An estimation approach that overcomes some of the drawbacks of previous approaches is the integration of inertial sensors with Global Positioning System (GPS) measurements. Researchers have demonstrated that a combination of GPS and inertial sensors can provide accurate measurements of slip angle [8], [9]. With knowledge of slip angle, cornering stiffness can be determined in the linear region of handling and both the coefficient of friction and cornering stiffness can be estimated in real-time [10]–[12]. Unfortunately, GPS-based approaches require satellite visibility, which may be lost periodically in urban and forested driving environments. Because the lateral tire force limits and tire slip angle can change rapidly with road surface conditions or during emergency maneuvers, during periods of GPS signal loss, it is important to be able to estimate these quantities *without* reliance on GPS.

Motivated by this necessity, researchers have considered a new source of information: steering torque. Steering torque measurements are readily available in vehicles with steer-by-wire, electric power steering (EPS), or active steering systems. From steering torque, total aligning moment (the moment generated about the steer axis by lateral tire force) can be extracted easily. Because aligning moment decreases well before tire force saturation, several approaches have been taken to utilize this information to improve vehicle stability. Nakajima demonstrated that steering torque can enhance ESC performance more than just relying on yaw rate measurements as an indication of vehicle instability [13]. Other algorithms have limited driver steering input once they detect a noticeable decrease in self-aligning torque [14]–[16]. These approaches unfortunately relied on linear observers for sideslip angle, which are only accurate away from the tire's lateral limits of adhesion. Even though all of these methods recognized

Manuscript received August 27, 2008; revised March 06, 2009; accepted July 11, 2009. Manuscript received in final form August 18, 2009. First published October 13, 2009; current version published June 23, 2010. Recommended by Associate Editor P. Meckl. This work was supported by Nissan Motor Corporation, Ltd. through funding the construction of the steer-by-wire vehicle P1.

The authors are with the Department of Mechanical Engineering, Stanford University, Stanford, CA 94305 USA (e-mail: judy.hsu@stanfordalumni.org; shadlaws@stanford.edu; gerdes@stanford.edu).

Color versions of one or more of the figures in this paper are available online at http://ieeexplore.ieee.org.

Digital Object Identifier 10.1109/TCST.2009.2031099

the value of total aligning moment as an early indication of exceeding the tire's lateral limits, none so far have provided explicit estimates of peak lateral force (or tire-road friction coefficient if normal force is known) and real-time estimates of tire slip angle.

This paper presents a new model-based estimation method that utilizes pneumatic trail information in steering torque to estimate tire slip angle (and thus vehicle sideslip angle) and the tire's lateral limits of adhesion. Based on simple models, the method relies on independent front steering torque measurements and other measurements which are readily available from automotive grade sensors. Most importantly, the innovation of this work is the recognition that the sensitivity of pneumatic trail to tire parameters even in the linear handling region enables early detection of peak lateral force *before* the limits are reached.

The first half of this paper develops the estimation framework. It motivates how total aligning moment can be used for tire force characterization and outlines the steering system model used in this work. It then describes the estimation algorithm, along with a proof of stability to demonstrate that the nonlinear estimator is stable in the presence of errors in the slip angle and the peak friction limits. The second half of the paper presents the experimental validation of the estimation method on a steer-by-wire research vehicle (pictured in Fig. 1). These results demonstrate the effectiveness of the algorithm in transient maneuvers near the friction limits and on a variable friction surface like loose gravel.

II. Identifying Lateral Limits of Adhesion

The motion of a vehicle is governed by the forces generated between the tire and the road. This section describes two concepts important for tire force characterization. First, we discuss how lateral tire force is generated as a function of tire deformation and present the tire model chosen for this work. Second, we motivate the benefits of pneumatic trail (the moment arm of the effective lateral force) for identifying the tire's lateral limit of adhesion.

A. Lateral Tire Force

Fig. 2 illustrates how lateral force is generated from tire deformation, both for a high friction and a low friction surface, assuming a parabolic pressure distribution in the contact patch. It depicts the tire traveling towards the right, starting on the left with zero lateral deformation (traveling straight) and ending on the right at the point where the required lateral force exceeds the available friction (skidding out of the page, towards the reader). The angle of tire deformation, or the difference between the tire's heading and velocity, is referred to as slip angle α. As slip angle increases, the lateral force distribution grows in area, which is represented by a shaded triangular area under the tire. However, the lateral force obtained is ultimately limited by the friction limit of the road, which is the product of the tire-road friction coefficient μ and the tire normal force F_z.

Plotting lateral force as a function of slip angle, we arrive at the tire curve presented in Fig. 3. Initially, lateral force is unaffected by the friction limits and grows nearly linearly according to the slope determined by cornering stiffness C_α. Ultimately,

Fig. 1. Experimental by-wire research vehicle P1.

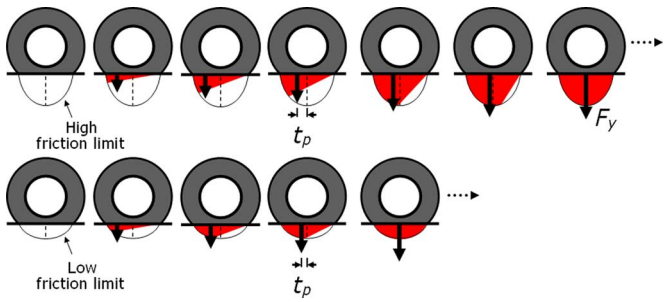

Fig. 2. Lateral force F_y generation as slip angle grows.

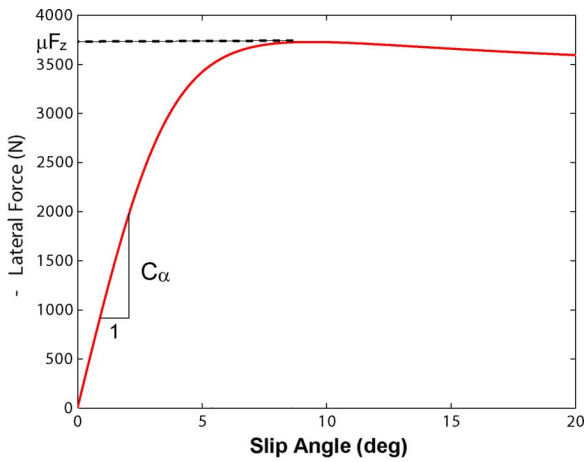

Fig. 3. Generic tire curve.

the force levels off due to the limit of tire adhesion μF_z. In practice, the exact shape and nuances of the curve are generally unknown. For example, on dry asphalt, there is a distinct peak to the tire curve, after which the force decreases slightly (as illustrated in Fig. 3) [6]. On dry gravel, experimental results demonstrate that the curve does not reach a distinct peak and simply levels off [17].

Numerous lateral tire force models exist. Commonly used models include a linear model which only depends on cornering stiffness and slip angle (which is only valid away from the friction limit), to the so-called Magic Formula model which is characterized by multiple empirical parameters [18]. In this work, we have chosen a simple nonlinear representation of a lateral tire force with a qualitative correspondence with experimental tire behavior. The brushed tire Fiala formula is a function of

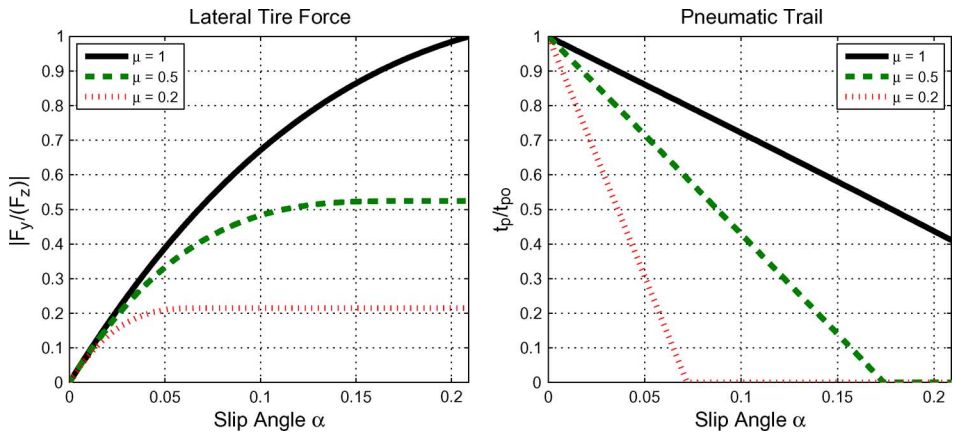

Fig. 4. Comparison of lateral force and pneumatic trail.

three fundamental physical tire parameters: cornering stiffness, normal force, and tire-road friction coefficient (which represents the ratio between the maximum lateral force to the normal force) [18]. It assumes no longitudinal forces, a parabolic pressure distribution, a rigid tire carcass, a constant coefficient of friction of sliding rubber, and neglects any dependence of cornering stiffness or friction on normal load

$$F_y = \begin{cases} -C_\alpha \tan\alpha + \frac{C_\alpha^2}{3}|\tan\alpha|\tan\alpha I_f, & \text{if } |\alpha| \le \alpha_{sl} \\ -\frac{C_\alpha^3}{27}\tan^3\alpha I_f^2 - \frac{1}{I_f}\text{sgn}\alpha, & \text{else} \end{cases} \quad (1)$$

where

$$\alpha_{sl} = \tan^{-1}\left(\frac{3}{C_\alpha I_f}\right) \qquad I_f = \frac{1}{\mu F_z}.$$

In the above formulation, α_{sl} is the slip angle at which the tire has lost lateral grip and I_f is referred to as the inverted peak friction limit. Also, with an estimate of cornering stiffness [8], I_f is the sole parameter to be estimated in this model. Estimation errors resulting from errors in the tire model can be bounded as discussed in Section V.

B. Pneumatic Trail

Returning our attention to Fig. 2, we observe that the effective lateral force F_y does not act directly at the center of the contact patch. Rather, F_y acts at a distance known as the tire pneumatic trail t_p, which induces a moment (known as self-aligning moment). As slip angle increases, F_y moves toward the center of the patch. This results in t_p vanishing once the force distribution reaches the limit of tire adhesion, the rate of which depends on the available peak friction.

The pneumatic trail can be derived analytically for a parabolic pressure distribution, however this is less accurate in practice than the accompanying force model [18]. As with the force model, we choose a simple representation and bound the resulting error in Section V. The model used here is an affine formula that begins at an initial trail length t_{po} and vanishes when the tires have lost lateral adhesion

$$t_p = \begin{cases} t_{po} - \frac{t_{po}C_\alpha}{3} I_f |\tan\alpha|, & \text{if } |\alpha| \le \alpha_{sl} \\ 0, & \text{else} \end{cases} \quad (2)$$

where t_{po} is derived to be $(1/6)l$ where l is the length of the tire contact patch by finding the centroid of the approximate triangular lateral force distribution in Fig. 2.

To demonstrate the benefits of pneumatic trail for tire property estimation, Fig. 4 plots the affine t_p model (normalized by t_{po}) and the Fiala tire model for various friction coefficients. For small angles, lateral force is relatively unaffected by the limit of tire adhesion, making it difficult to distinguish between different friction limits before the limits are reached. However, pneumatic trail is sensitive to the friction limit μF_z even when lateral force is in the linear region of handling, offering the potential to enable early prediction of the tire's handling limits.

C. Total Aligning Moment

Although pneumatic trail is valuable for tire property estimation, it is generally not known and must be estimated. Fortunately, the moment generated about the steer axis from lateral force, referred to as total aligning moment, contains pneumatic trail information and is available. Below, we present a simple model for total aligning moment.

Introduced previously, self-aligning moment is generated by lateral force acting at a moment arm defined as the pneumatic trail. Supplementing this, the steering system geometry also provides an additional lever arm for lateral force. Because the steer axis is normally not vertical, nor is it in line with the point of tire contact with the ground, it provides lateral force with a lever arm called the mechanical (caster) trail t_m. Mechanical trail is a function of steering geometry and can be determined by kinematics [19], [20]. Thus, the moment produced by lateral force in the steering system, referred to as total aligning moment τ_a, is the result of the force acting at a distance $(t_p + t_m)$

$$\tau_a = -(t_m + t_p)F_y. \quad (3)$$

Combining the Fiala lateral tire force, mechanical trail and linear pneumatic trail models in (2) yields the following total aligning moment model before the tires are fully sliding:

$$\tau_a = -\left(t_m + t_{p0} - \frac{t_{p0}C_\alpha}{3}|\tan\alpha| I_f\right) \cdot \left(-C_\alpha \tan\alpha + \frac{C_\alpha^2}{3}|\tan\alpha|\tan\alpha I_f - \frac{C_\alpha^3}{27}\tan^3\alpha I_f^2\right). \quad (4)$$

After full sliding, total aligning moment reduces to

$$\tau_a = \frac{t_m}{I_f}\text{sgn}\alpha. \tag{5}$$

In a steering system, there are multiple sources contributing to the overall torque in the system. In order to extract total aligning moment from the various contributions of torque in the steering system, the next section develops detailed models for the individual torques and forces in a steer-by-wire steering system.

III. Steering System Model

The following steering model is developed for the research vehicle considered in this study, P1 (see Fig. 1) [19]. Built at Stanford University, P1 has independent front steering steer-by-wire capability. The derivation outlines the steering dynamics for an individual front tire, although a similar process could be applied to vehicles with a mechanical steering linkage between the front tires. It could also be applied to production EPS and active steering systems by including the driver commanded torque contribution, which is an available measurement from the on-board torque sensor on the steering column [6].

It is our objective to keep the steering system model as simple as possible while ensuring that it captures the important characteristics of the system. With a steer-by-wire system, the total torque about the steer axis τ is

$$\tau = \tau_a + \tau_j + \tau_{\text{act}} \tag{6}$$

where total aligning moment τ_a is the net torque resulting from lateral tire forces, jacking torque τ_j is the resulting torque from the vertical tire forces, and τ_{act} is the torque generated by the steering motor. For simplicity, the torque generated from longitudinal tire forces acting through the scrub radius is neglected, although the inclusion of longitudinal forces may be considered for future work. Expressions for jacking torque τ_j and net actuated motor torque τ_{act} are derived below.

A. Jacking Torque τ_j

Jacking torque is the reaction torque produced from the vertical tire force and suspension travel as a function of steer angle δ. It is a function of suspension geometry and can be modeled as

$$\tau_j(\delta) = F_z\frac{dh}{d\delta}(\delta) \tag{7}$$

where h is the change in suspension height due to steering, which is known from kinematics [19].

Lateral Load Transfer: In order to account for the effects of lateral load transfer on the front tires, which affects the amount of jacking torque, we use the following steady-state weight transfer model. Summing the moments about the front roll center yields a change in load at the front tires ΔF_z

$$\Delta F_z = \frac{1}{t_f}\left(K_{\phi f}\phi + h_f a_y\frac{2F_{\text{znom}}}{g}\right) \tag{8}$$

where t_f is the front vehicle track width, $K_{\phi f}$ is the front roll stiffness, ϕ is the roll angle, h_f is the height of the front roll center, g is the acceleration due to gravity, and a_y is the lateral acceleration. Equation (8) assumes that the left and right tires begin with the same nominal load F_{znom}.

From (8), the loads on the front left and right tires, F_{zl} and F_{zr}, are

$$F_{zl} = F_{\text{znom}} - \Delta F_z \tag{9}$$

$$F_{zr} = F_{\text{znom}} + \Delta F_z. \tag{10}$$

The following section develops steer-by-wire actuated motor torque, the remaining piece in the overall system model for a steer-by-wire system.

B. Actuated Motor Torque τ_{act}

The motor torque τ_{act} includes the commanded motor current i, gearbox ratio n_g, motor constant k_m, Coulomb friction in the motor assembly f_m and steering system f_w which are nonlinear functions of the steer angle direction, gearbox efficiency η, and linkage ratio of the steering system n_l [19]

$$\tau_{\text{act}} = \left(n_g k_m i - f_m(\dot{\delta})\right)\eta n_l - f_w(\dot{\delta}). \tag{11}$$

A complete steering model for a given tire includes the effective damping b_{eff} and inertia J_{eff}, yielding

$$J_{\text{eff}}\ddot{\delta} + b_{\text{eff}}\dot{\delta} = \tau_a + \tau_j + \tau_{\text{act}}. \tag{12}$$

In order to extract the total aligning torque from the steering system model developed above, a linear Luenberger disturbance observer was developed in [20]. This estimated total aligning torque is then used as a measurement for pneumatic trail nonlinear observer presented in the next section.

IV. Pneumatic Trail Nonlinear Observer

A. Estimation Concept

Conceptually, the estimation method comprises two main blocks: the slip angle observer and the friction and force estimator (see Fig. 5). While the estimation approach outlined here is tailored for the independent left/right steering system of P1, the algorithm is adaptable to conventionally linked steering systems. As shown in the block diagram, both estimation blocks rely on each other's estimates to output their own estimates. Due its highly coupled nature, care must be taken to ensure that errors in either α or μF_z estimates do not cause the entire observer to grow unstable, an issue that is discussed in the stability proof that follows.

B. Vehicle Model

To estimate tire slip angle, we use a model for how vehicle sideslip angle evolves as a function of the lateral tire forces. The vehicle is modeled using a planar single-track bicycle model (see Fig. 6) with nonlinear front and rear tire forces, F_{yf} and F_{yr}, described in (1)

$$\dot{\beta} = \frac{1}{mV_x}(F_{yf} + F_{yr}) - r \tag{13}$$

$$\dot{r} = \frac{1}{I_z}(aF_{yf} - bF_{yr}) \tag{14}$$

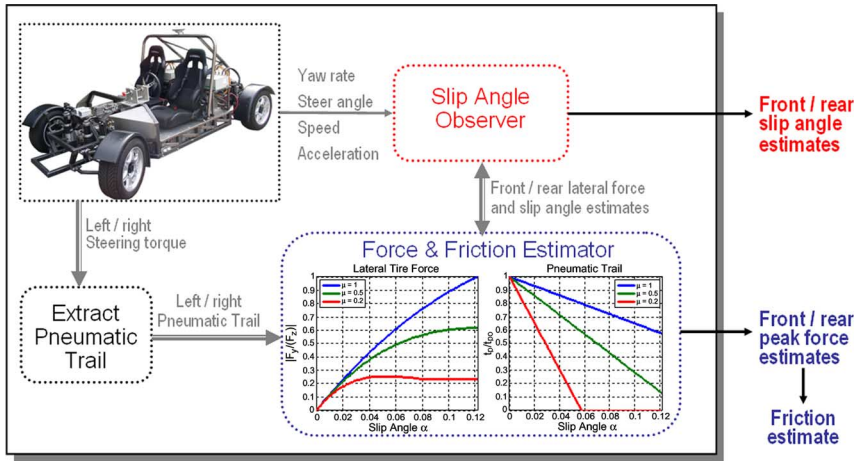

Fig. 5. Pneumatic trail nonlinear observer block diagram.

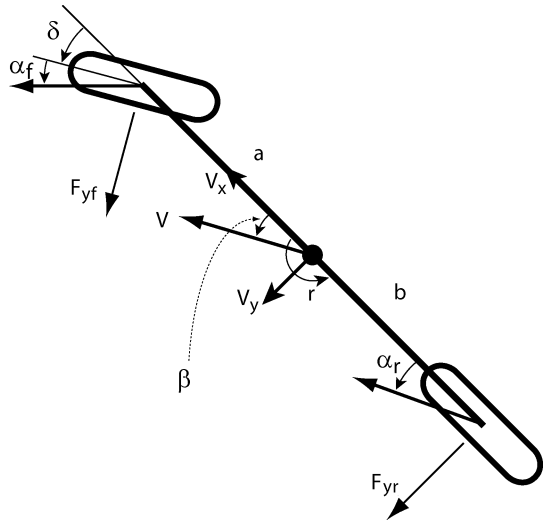

Fig. 6. Bicycle model.

where a and b are the distances of the front and rear axles from the CG, sideslip angle β is the angle between the vehicle's heading and the direction of its velocity, r is the yaw rate, I_z is the moment of inertia, m is the vehicle mass, V_x is the longitudinal vehicle speed. Using kinematics, the front and rear tire slip angles are linearized to be

$$\alpha_f = \beta + \frac{ar}{V_x} - \delta \tag{15}$$

$$\alpha_r = \beta - \frac{br}{V_x} \tag{16}$$

where δ is the steer angle at the tire.

C. Real-Time Estimation Algorithm

Prior to beginning estimation, the initial front axle slip angle $\widehat{\alpha}_{fo}$ is set to zero (i.e., the vehicle is driving straight) and inverted front peak lateral force $\widehat{I}_{fo}$ is initialized to

$$I_{\text{fnom}} = \frac{1}{\mu_{\text{nom}} F_{\text{zfnom}}} \tag{17}$$

where the nominal friction coefficient $\mu_{\text{nom}} = 1$, and F_{zfnom} is the nominal front axle load. The estimation algorithm is as follows.

1) **Form estimates of lateral force.**
With an estimate of front slip angle, the rear slip angle estimate is obtained by combining (15) and (16)

$$\widehat{\alpha}_r = \widehat{\alpha}_f + \delta - \frac{(a+b)r}{V_x} \tag{18}$$

where δ is measured from onboard steering encoders, r is measured from onboard INS, and V_x is determined by wheel speed sensors.
Assuming that the vehicle is traveling on an even road surface, the friction coefficients for the front and rear axles are assumed to be equal. Neglecting the effects of longitudinal weight transfer, the inverted rear axle peak force is

$$\widehat{I}_r = \frac{\widehat{I}_f F_{\text{zfnom}}}{F_{\text{zrnom}}} \tag{19}$$

where F_{zrnom} is the nominal rear axle load and $\widehat{I}_f$ is the inverted front axle peak force estimate. Using the Fiala tire force model in (1), the rear axle force $\widehat{F}_{yr}$ is calculated based on the current estimates $\widehat{I}_r$ and $\widehat{\alpha}_r$. For the front lateral force $\widehat{F}_{yf}$, we treat the left and right tires separately and sum their lateral force contributions

$$\widehat{F}_{yf} = \widehat{F}_{yfl} + \widehat{F}_{yfr} \tag{20}$$

where $\widehat{F}_{yfl}$ and $\widehat{F}_{yfr}$ are calculated using (1) based on $\widehat{\alpha}_f$ and their respective friction limit estimates.

2) **Update estimates of front/rear slip angle.**
The update equation for the front slip angle is derived by taking the derivative of (15) and substituting in (13), (14)

$$\dot{\alpha}_f = \left(\frac{1}{mV_x} + \frac{a^2}{I_z V_x}\right) F_{yf} + \left(\frac{1}{mV_x} - \frac{ab}{I_z V_x}\right) F_{yr} - r - \dot{\delta}. \tag{21}$$

Thus, to update $\widehat{\alpha}_f$, we may integrate the following observer update law:

$$\dot{\widehat{\alpha}}_f = \left(\frac{1}{mV_x} + \frac{a^2}{I_z V_x}\right) \widehat{F}_{yf} + \left(\frac{1}{mV_x} - \frac{ab}{I_z V_x}\right) \widehat{F}_{yr} - r - \dot{\delta} + K(\widehat{F}_{yf} + \widehat{F}_{yr} - ma_y) \tag{22}$$

where K is the observer feedback gain and a_y is the lateral acceleration measurement. However, to avoid having to take the derivative of the measured steer angle signal δ, we rearrange the update equation as

$$\dot{\widehat{\alpha}}_f + \dot{\delta} = \left(\frac{1}{mV_x} + \frac{a^2}{I_z V_x}\right)\widehat{F}_{yf} + \left(\frac{1}{mV_x} - \frac{ab}{I_z V_x}\right)\widehat{F}_{yr} - r + K(\widehat{F}_{yf} + \widehat{F}_{yr} - ma_y). \tag{23}$$

We may integrate this update equation instead and subtract away δ after integration. Once $\widehat{\alpha}_f$ is updated, it is straightforward to update the rear slip estimate $\widehat{\alpha}_r$ from the kinematic relationship described in (18).

3) **Form pneumatic trail estimate.**
In this step, we consider the front tires separately. To construct an estimated left pneumatic trail $\widehat{t}_{pl}$ for the left tire, we use the measured total aligning moment for the left tire τ_{al} extracted from the disturbance observer designed in [20] and lateral force estimate $\widehat{F}_{yfl}$

$$\widehat{t}_{pl} = -\left(\frac{\tau_{al}}{\widehat{F}_{yfl}} + t_{ml}\right) \tag{24}$$

where the left mechanical trail t_{ml} is determined kinematically as a function of the measured steer angle [19].
For the right tire, we perform an analogous calculation to construct an estimated right pneumatic trail $\widehat{t}_{pr}$.
A three-point moving average filter is included in the calculations of $\widehat{t}_{pl}$ and $\widehat{t}_{pr}$ to prevent the dynamics of the estimates from changing faster than the physical system. (The length of the filter can be adjusted according to the system's sampling rate and level of sensor measurement noise.)

4) **Use pneumatic trail to solve for peak lateral force.**
From the pneumatic trails, the linear model in (2) is used to solve for the estimated inverted peak lateral force of the left and right tires, $\widehat{I}_{fl}$ and $\widehat{I}_{fr}$, respectively. Before full sliding ($\widehat{\alpha}_f < \widehat{\alpha}_{fsl}$), the estimates are

$$\widehat{I}_{fl} = \frac{3(t_{po} - \widehat{t}_{pl})}{t_{po} C_{\alpha fl} |\tan\widehat{\alpha}_f|} \tag{25}$$

$$\widehat{I}_{fr} = \frac{3(t_{po} - \widehat{t}_{pr})}{t_{po} C_{\alpha fr} |\tan\widehat{\alpha}_f|} \tag{26}$$

where t_{po} is the initial pneumatic trail length and $C_{\alpha fl}$ and $C_{\alpha fr}$ are the front left and right tire cornering stiffnesses, respectively. After full sliding ($\widehat{\alpha}_f \geq \widehat{\alpha}_{fsl}$), the inverted peak force estimates are

$$\widehat{I}_{fl} = \frac{t_{ml}}{\tau_{al}} \mathrm{sgn}\widehat{\alpha}_f \tag{27}$$

$$\widehat{I}_{fr} = \frac{t_{mr}}{\tau_{ar}} \mathrm{sgn}\widehat{\alpha}_f. \tag{28}$$

Finally, we may lump the left/right peak forces to find the front axle peak force estimate, $1/\widehat{I}_f$

$$\frac{1}{\widehat{I}_f} = \frac{1}{\widehat{I}_{fl}} + \frac{1}{\widehat{I}_{fr}}. \tag{29}$$

We emphasize that the strength of this estimation method lies in the fact that pneumatic trail provides sufficiently early information of the limit of tire adhesion *before* they affect lateral tire force generation (and therefore would alter our slip angle estimates). While initially operating in the linear region of handling, slip angle is approximately proportional to cornering stiffness. This enables accurate tracking of slip angle even when we have insufficient knowledge of the limits of tire adhesion. Pneumatic trail conveniently provides knowledge of the friction limit before the tires exit the linear region of handling, and we are able to continue accurate slip angle tracking up to the limits of handling.

D. Experimental Implementation Considerations

To interpret the performance of the observer, it may be desirable to know the tire-road coefficient of friction estimate $\widehat{\mu}$, rather than peak lateral force. Given the prior assumption that longitudinal weight transfer is negligible and the vehicle is traveling on an even surface, $\widehat{\mu}$ is derived directly from the peak force estimate of the front axle

$$\widehat{\mu} = \frac{1}{\widehat{I}_f F_{\mathrm{zfnom}}}. \tag{30}$$

The final friction coefficient estimate may be put through a 100-point moving average filter to obtain smoother estimates, which for a 500 Hz sampling rate translates to the assumption that the road friction can change as quickly as every 0.2 s.

For onboard implementation, when the vehicle is traveling straight or nearly straight, we remember that lateral limit estimation is imprecise given the lack of lateral dynamics. During these situations, we should suspend peak force (friction) estimation, holding it at its latest known or nominal value. Quantitatively, this translates to waiting to observe a decrease in pneumatic trail from its initial value ($\widehat{t}_p < t_{po}$) and a slip angle bounded away from zero ($|\widehat{\alpha}_f| > \alpha_{\mathrm{thres}}$) before the peak force estimation can be meaningful.

Because the slip angle is expected to change at a frequency of 1–5 Hz, the total aligning moment measurement should be low-pass filtered at the tire hop frequency ($f = 10 - 15$ Hz) to prevent the high frequency road disturbances from being propagated to the slip angle estimate. For consistency, the slip angle estimates should be low-pass filtered at the same frequency. Other signals such as yaw rate and lateral acceleration should be similarly conditioned prior to using them in the algorithm. Finally, in order to use the load transfer model in (8), we require knowledge of roll angle. For convenience, roll angle measurements and roll stiffness are obtained through a combination of onboard GPS and INS measurements [9]. However, in the absence of GPS, Tseng has shown that one can separate lateral dynamics from road disturbances to obtain accurate roll angle measurements in dynamic maneuvers [21].

V. Pneumatic Trail Nonlinear Observer Stability Proof

Consider a front slip angle error defined as

$$e_\alpha = \widehat{\alpha}_f - \alpha_f \tag{31}$$

where α_f is the actual (unknown) front slip angle.

Suppose the following three conditions hold.

1) The error due to lateral force modeling errors and parameter uncertainty is bounded by a maximum force error ΔF_y.
2) The local cornering stiffnesses of the front and rear axles, $\widetilde{C}_{\alpha f}$ and $\widetilde{C}_{\alpha r}$, are not both zero (meaning the vehicle is not in a full lateral skid) and the observer feedback gain K is chosen such that

$$K > \left| \frac{1}{mV_x} - \frac{ab}{I_z V_x} \right|. \tag{32}$$

3) Let us define the nonlinear handling region as

$$|F_{yf} - F_{yflin}| \geq \Delta F_y \tag{33}$$
$$|F_{yr} - F_{yrlin}| \geq \Delta F_y \tag{34}$$

where the linear forces are approximated by

$$F_{\text{yflin}} = -C_{\alpha f}\alpha_f \tag{35}$$
$$F_{\text{yrlin}} = -C_{\alpha r}\alpha_r. \tag{36}$$

When the tires are operating in this region, the error in the estimated pneumatic trail $\widehat{t}_p$ (for both the front left and right tires) is bounded by

$$|\widehat{t}_p - t_p| < \frac{t_{po} C_{\alpha f} I_f}{3} \frac{K \Delta F_y}{\gamma} \tag{37}$$

where t_p is the actual (unknown) pneumatic trail and

$$\gamma = K_f \widetilde{C}_{\alpha f} + (K_r + K)\widetilde{C}_{\alpha r}$$
$$K_f = \frac{1}{mV_x} + \frac{a^2}{I_z V_x}$$
$$K_r = \frac{1}{mV_x} - \frac{ab}{I_z V_x}.$$

Then, as the following proof shows, the slip angle estimation error is stable and bounded by

$$|e_\alpha| \leq \frac{K\Delta F_y}{\gamma} = \frac{K\Delta F_y}{K_f \widetilde{C}_{\alpha f} + (K_r + K)\widetilde{C}_{\alpha r}}. \tag{38}$$

In the special case where we have perfect knowledge of lateral force ($\Delta F_y = 0$), then asymptotic stability of the slip angle estimation error is guaranteed, i.e., $\widehat{\alpha}_f \to \alpha_f$ and $\widehat{\alpha}_r \to \alpha_r$ as $t \to \infty$.

Proof: For asymptotic stability [22], we would like to show a positive real γ exists such that

$$\dot{e}_\alpha \leq -\gamma e_\alpha. \tag{39}$$

By taking the derivative of (31) and substituting in the front slip angle update law from the nonlinear observer, the slip angle estimation error dynamics are

$$\dot{e}_\alpha = \dot{\widehat{\alpha}}_f - \dot{\alpha}_f \tag{40}$$

$$= \underbrace{\left(\frac{1}{mV_x} + \frac{a^2}{I_z V_x} \right)}_{K_f} (\widehat{F}_{yf} - F_{yf}) + \underbrace{\left(\frac{1}{mV_x} - \frac{ab}{I_z V_x} \right)}_{K_r} (\widehat{F}_{yr} - F_{yr}) + K(\widehat{F}_{yf} + \widehat{F}_{yr} - ma_y). \tag{41}$$

As the lateral force estimation error is bounded by ΔF_y (Condition 1), we may rewrite the feedback term in (41) as

$$K(\widehat{F}_{yf} + \widehat{F}_{yr} - ma_y) = K(\widehat{F}_{yr} - F_{\text{yrmeas}}) \tag{42}$$

where

$$F_{\text{yrmeas}} = ma_y - \widehat{F}_{yf} \tag{43}$$
$$|F_{\text{yrmeas}} - F_{yr}| \leq \Delta F_y. \tag{44}$$

Now (41) can be rewritten as

$$\dot{e}_\alpha \leq K_f(\widehat{F}_{yf} - F_{yf}) + (K_r + K)(\widehat{F}_{yr} - F_{yr}) + K\Delta F_y. \tag{45}$$

Without loss of generality, assume that $\widehat{\alpha}_f > 0$. Then, let us consider the following two possible cases of estimation error:

Case 1) slip angle estimate is greater or equal than actual;

Case 2) slip angle estimate is less than actual.

In keeping with the original goal stated in (39), we would like to show that for both cases, the force errors $(\widehat{F}_{yf} - F_{yf})$ and $(\widehat{F}_{yr} - F_{yr})$ in (45) can be bounded by the slip angle estimation error.

Case 1: Consider the first case in which the estimation error is nonnegative, i.e., $\widehat{\alpha}_f \geq \alpha_f$. Given the pneumatic trail estimates for the front left and right tires, $\widehat{t}_{pl}$ and $\widehat{t}_{pr}$, respectively, the algorithm algebraically solves for estimated friction limits $1/\widehat{I}_{fl}$ and $1/\widehat{I}_{fr}$ using the current estimate of front slip angle. With $\widehat{\alpha}_f \geq \alpha_f$ and Condition 3 satisfied, we see that for the front left tire

$$\frac{1}{\widehat{I}_{fl}} = \frac{t_{po} C_{\alpha fl} |\tan \widehat{\alpha}_f|}{3(t_{po} - \widehat{t}_{pl})} \tag{46}$$
$$\geq \frac{t_{po} C_{\alpha fl} |\tan \alpha_f|}{3(t_{po} - t_{pl})} = \frac{1}{I_{fl}}. \tag{47}$$

That is, an overestimated slip angle yields an overestimated friction limit. This effect is illustrated graphically in Fig. 7 with $\alpha_f = \alpha_1$ and $\widehat{\alpha}_f = \alpha_2$ (and $\widehat{t}_p = t_p$ for illustration purposes). Similarly, the friction limit is overestimated for the front right tire. This results in a lateral axle force estimate $\widehat{F}_{yf}$ which is negative and larger in magnitude than the actual force (recalling that positive slip angle produces negative lateral force).

Now, the error in (45) can be bounded by

$$\dot{e}_\alpha \leq -K_f \widetilde{C}_{\alpha f}(\widehat{\alpha}_f, \widehat{I}_f)(\widehat{\alpha}_f - \alpha_f) - (K_r + K)\widetilde{C}_{\alpha r}(\widehat{\alpha}_r, \widehat{I}_r)(\widehat{\alpha}_r - \alpha_r) + K\Delta F_y. \tag{48}$$

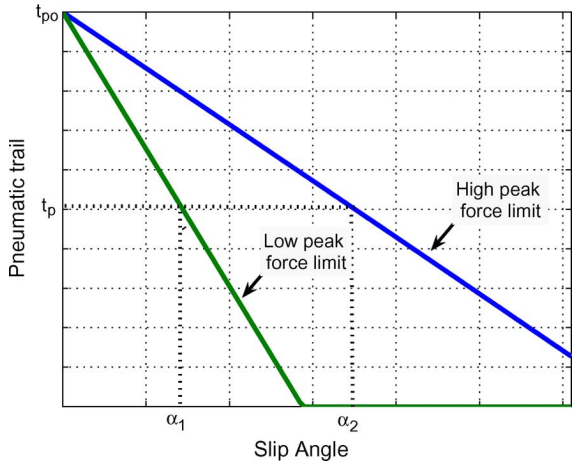

Fig. 7. Calculating force limit from pneumatic trail.

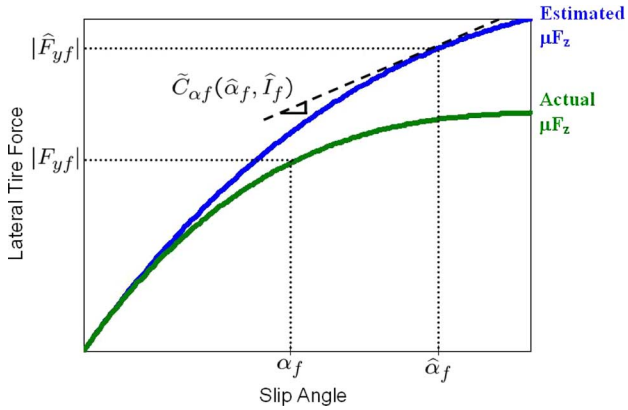

Fig. 8. Bounding lateral force error when $\hat{\alpha}_f > \alpha_f$.

The upper bound in (48) follows from nature of Fiala tire model. The modeled tire curve is not only Lipshitz continuous, but as slip angle increases, the magnitude of the local first derivative (e.g., local cornering stiffness) also decreases. Because $\hat{\alpha}_f \geq \alpha_f$, extrapolating the local stiffness at $\hat{\alpha}_f$ for the front axle provides a bound for the error in the force estimate (the magnitude of the estimated force error is always less than $\widetilde{C}_{\alpha f}$ multiplied by the slip angle error). This bound is admittedly conservative, yet can be easily understood from Fig. 8. A similar bound is derived for the rear axle lateral force error using the rear local cornering stiffness $\widetilde{C}_{\alpha r}$.

Recalling that the rear slip angle is kinematically linked to the front slip angle by (18), we see that rear slip angle error is in fact equivalent to front slip angle error

$$\hat{\alpha}_r - \alpha_r = \hat{\alpha}_f - \alpha_f \tag{49}$$

and (48) can be further simplified to be

$$\dot{e}_\alpha \leq -\left[K_f \widetilde{C}_{\alpha f}(\hat{\alpha}_f, \hat{I}_f) + (K_r + K)\widetilde{C}_{\alpha r}(\hat{\alpha}_r, \hat{I}_r)\right] e_\alpha + K\Delta F_y. \tag{50}$$

Case 2: The second case considers a negative estimation error. Now with $\hat{\alpha}_f < \alpha_f$, the observer *underestimates* the friction limit for the front left and right tires using (26), an effect shown in Fig. 7 (here, $\hat{\alpha}_f = \alpha_1$ and $\alpha_f = \alpha_2$). This produces

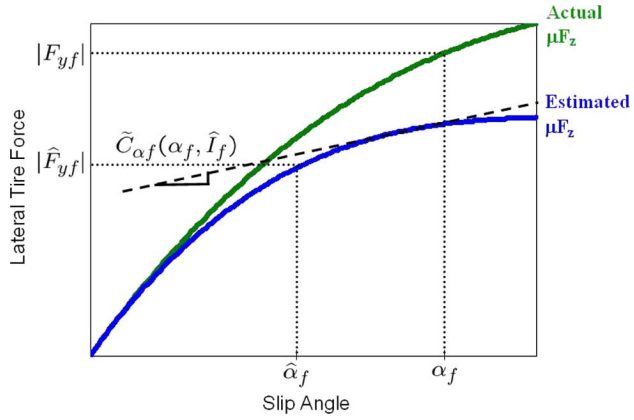

Fig. 9. Bounding lateral force error when $\hat{\alpha}_f < \alpha_f$.

a lateral axle force estimate $\hat{F}_{yf}$ which is smaller in magnitude than the actual force, illustrated in Fig. 9. Now, the error dynamics are

$$\dot{e}_\alpha \leq -\left[K_f \widetilde{C}_{\alpha f}(\alpha_f, \hat{I}_f) + (K_r + K)\widetilde{C}_{\alpha r}(\alpha_r, \hat{I}_r)\right] e_\alpha + K\Delta F_y. \tag{51}$$

Note that in order to use the local stiffness to bound the force residual for either case, we must use the smaller local stiffnesses $\widetilde{C}_{\alpha f}(\alpha_f, \hat{I}_f)$ and $\widetilde{C}_{\alpha r}(\alpha_r, \hat{I}_r)$ corresponding to the larger slip angle.

Putting the two cases together, we have nearly satisfied the desired error dynamics for stability. The slip angle error dynamics are

$$\dot{e}_\alpha \leq -\gamma e_\alpha + K\Delta F_y \tag{52}$$

where

$$\gamma = K_f \widetilde{C}_{\alpha f} + (K_r + K)\widetilde{C}_{\alpha r}$$
$$\widetilde{C}_{\alpha f} = -\left.\frac{dF_{yf}}{d\alpha_f}\right|_{\left(\max\{\alpha_f, \hat{\alpha}_f\}, \hat{I}_f\right)}$$
$$\widetilde{C}_{\alpha r} = -\left.\frac{dF_{yr}}{d\alpha_r}\right|_{\left(\max\{\alpha_r, \hat{\alpha}_r\}, \hat{I}_r\right)}.$$

Now, because Condition 2 ensures that γ is a real, positive number, the slip angle estimation error is simply bounded by the uncertainty in lateral force ΔF_y from the error dynamics equation in (52)

$$|e_\alpha| \leq \frac{K\Delta F_y}{\gamma} = \frac{K\Delta F_y}{K_f \widetilde{C}_{\alpha f} + (K_r + K)\widetilde{C}_{\alpha r}}. \tag{53}$$

In the special case where we have perfect knowledge of lateral force ($\Delta F_y = 0$), asymptotic stability of the observer can be guaranteed. Let $V(e_\alpha) = (1/2)e_\alpha^2$ be a candidate Lyapunov function. Then

$$\dot{V}(e_\alpha) = e_\alpha \dot{e}_\alpha \tag{54}$$
$$\leq -\gamma e_\alpha^2. \tag{55}$$

So $-\dot{V}(e_\alpha)$ is greater than a positive definite function, which implies asymptotic stability and guarantees $\hat{\alpha}_f \to \alpha_f$ (and $\hat{\alpha}_r \to \alpha_r$) as $t \to \infty$.

A. Stability Proof Remarks

1) Remarks for Condition 2: Condition 2 arises from the fact that we require that $\gamma > 0$ in (52) in order to ensure that the slip angle error is bounded. The first implication of this condition is that the observer is stable if either the front *or* rear axle forces have reached their peaks, but not both. From an estimation standpoint, this fundamentally makes sense. For example, one could imagine that immediately after the vehicle loses lateral traction, sideslip angle grows from a relatively small angle to a larger angle corresponding to a full skid, all of which occurs under saturated front and rear lateral forces.

Although the slip angles are unobservable during situations of complete loss of lateral traction, the larger aim of this work is to incorporate the nonlinear observer into a stability control scheme. Fortunately, regardless of the magnitude of the tire slip angles, during a full sideways skid the control aim is unambiguous—the controller should utilize available actuators to reduce slip angle and counteract the skid.

Condition 2 conveniently provides a minimum value for the observer feedback gain as a function of vehicle speed. Furthermore, (52) suggests that the effect of gain K on the estimation convergence rate is most dominant when the front tires have saturated, and is least significant when the front tires retain lateral traction, an effect that has been confirmed experimentally.

2) Remarks for Condition 3: In the linear handling region (when the lateral force can be well approximated by $F_y = -C_\alpha \alpha$), the observer is stable regardless of the accuracy of pneumatic trail. Once the actual lateral forces enter the nonlinear region, we may derive the required accuracy of our knowledge of pneumatic trail stated in Condition 3. In the discussion that follows, we consider the linear and nonlinear regimes separately. We also assume $\widehat{\alpha}_f > \alpha_f$, yet a similar argument can be made when $\widehat{\alpha}_f < \alpha_f$.

Linear Handling Region: If the estimated lateral forces $\widehat{F}_{yf}$ and $\widehat{F}_{yr}$ are well approximated by a linear tire model [they also satisfy (33), (34)], then we can write the slip angle error dynamics from (45) as

$$\dot{e}_\alpha = -\left[K_f C_{\alpha f} + (K_r + K) C_{\alpha r}\right] e_\alpha + K \Delta F_y \tag{56}$$

where the lateral force residuals are bounded by their linear cornering stiffnesses, which are indeed independent from the pneumatic trail estimate.

Even when $\widehat{F}_{yf}$ and $\widehat{F}_{yr}$ are nonlinear, the observer is guaranteed stable even with an imperfect pneumatic trail measurement. In this situation, we can use the local cornering stiffnesses to arrive at the same bound as before in (52). Naturally, the observer obtains faster estimation convergence with a more accurate estimate of the friction limits. However, regardless of the accuracy of pneumatic trail, the observer is always stable and the error is bounded when the actual lateral forces are in the linear region.

Nonlinear Handling Region: If the actual lateral forces generated at the tires are in the nonlinear region of operation, then we require a certain level of accuracy of our pneumatic trail information for observer stability. In order to use the local cornering stiffness as a valid bound on the slip angle estimation error, an overestimated (underestimated) slip angle must produce an overestimated (underestimated) friction limit, shown in Fig. 7. Thus, for either tire, the slip angle error dynamics are stable and bounded if

$$|\widehat{t}_p - t_p| < \frac{t_{po} C_{\alpha f} I_f}{3} |\tan \widehat{\alpha}_f - \tan \alpha_f|. \tag{57}$$

Approximating for small angles and substituting the error bound from (52), we have

$$|\widehat{t}_p - t_p| < \frac{t_{po} C_{\alpha f} I_f}{3} \frac{K \Delta F_y}{\gamma}. \tag{58}$$

Conceptually, this condition states that the observer requires pneumatic trail information that is more accurate than its estimate of front slip angle. This is reasonable since pneumatic trail is a measurement to adjust the tire curve properties used to update the front slip angle estimate.

The most stringent condition on our accuracy of pneumatic trail information is when both tires have just exited the linear region on a high friction surface. As the local cornering stiffnesses decrease (as forces transition to saturation region), or as the friction coefficient or tire normal load decreases, the allowable error for stability increases. Thus, the observer requires less precise knowledge of pneumatic trail when the vehicle is driving on a slippery surface, or on the inside tire during a turn, both of which are important situations that require tire parameter knowledge.

VI. Experimental Results

In order to test the performance of the estimation method, vehicle test runs were performed on P1. P1 is equipped with a sensor suite that includes steering encoders, a GPS system that measures vehicle sideslip and roll angles, and automotive-grade gyroscopes and lateral accelerometers. To validate the observer on two different coefficient of friction values, vehicle test runs were conducted on two types of surfaces: dry pavement ($\mu = 1$) and loose gravel ($\mu = 0.5$ to 0.7). Both testing surfaces are flat.

A. Pavement Experimental Results

First, a quasi-steady-state ramp steer is performed on pavement with P1, shown in Fig. 10(a). Driven at a constant speed of 10 m/s, this maneuver achieves full lateral force saturation of the front tires. Using the estimation algorithm, the resulting friction and slip angle estimates are shown in Fig. 10(b). The friction estimate holds steadily at $\mu = 1$, which agrees with skidpad testing. At $t = 6.5$ s, the vehicle travels over a slippery metal grate, which prompts the friction estimate to correctly decrease momentarily. Note that the tire-road friction is predicted when vehicle has achieved only 50% of its peak lateral force.

The front and rear slip angle estimates are compared with GPS-based measurements, which are taken as truth [9], and with the linear slip angle feedback observer which assumes $F_y = -C_\alpha \alpha$ and uses lateral acceleration and yaw rate as measurements [23]. In the linear region of handling, as expected, both observers match well with GPS-based measurements. However, after the vehicle enters nonlinear region of handling (after $t = 6$ s), the limitations of a linear sideslip estimator are clearly evident as large errors begin to develop. Meanwhile, the slip angle estimates for the pneumatic trail-based estimator are comparable to those from GPS well into the nonlinear region of han-

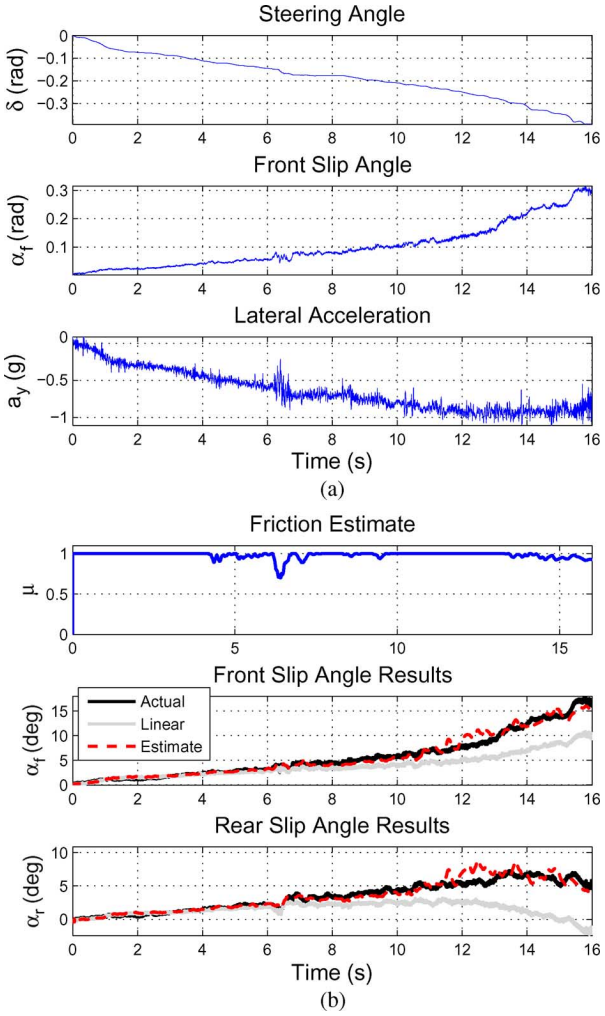

Fig. 10. Experimental ramp steer (pavement). (a) Maneuver. (b) Estimation results.

dling. This demonstrates that the simple total aligning moment model proposed in this work has reasonable correspondence to experiment. After $t = 12$ s, the front lateral tire force has fully saturated. However, the estimate is still able to track GPS-based measurements reasonably well since the rear tire forces have yet to reach full saturation (from Condition 2 in Section V).

The second maneuver presented is a slalom at a constant speed of 15 m/s which intermittently enters the nonlinear operating region of the tires [see Fig. 11(a)]. The slip angle estimates for this maneuver are shown in Fig. 11(b). Again, as expected, both estimators match well with GPS-based measurements in the linear handling region. However, when the vehicle enters the nonlinear handling region (near $t = 4$ and 12 s), the benefit of the pneumatic trail-based estimation approach over the linear estimator is evident. The former tracks the actual slip angle better and is within the accuracy of the GPS measurement.

The friction estimate is around the correct value of $\mu = 1$ during the majority of the maneuver. The slight deviation in the friction estimate during this quickly changing steering command is a function of slip angle estimation error propagating to the peak force estimate when the magnitude of front slip angle is small. Given sufficient lateral dynamics, however, the friction estimate matches well with truth. This experimental slalom maneuver demonstrates that the speed of the observer response is adequate for accurate tire characterization during fast steering maneuvers.

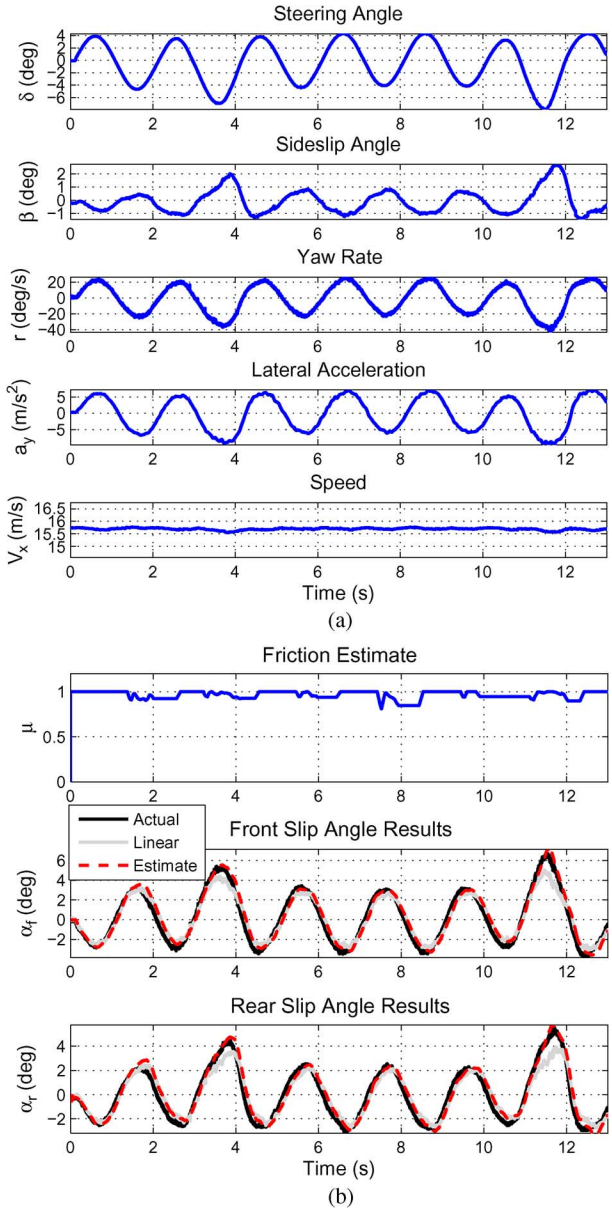

Fig. 11. Experimental slalom (pavement). (a) Maneuver time history. (b) Estimation results.

B. *Gravel Experimental Results*

Shown in Fig. 12(a), the third maneuver presented is a series of sharp transient turns performed on a loose gravel course. Driven at an average speed of 9 m/s, this maneuver pushes the front tires well into the saturation region. Fig. 12(b) illustrates the observer performance. The friction estimates hold at the nominal value of $\mu = 1$ during periods of insufficient lateral excitation, and reach a value of $\mu = 0.5$ to 0.6 when the vehicle is turning. This friction coefficient estimate on this gravel surface is quite reasonable given that the front tires are almost completely skidding.

With this maneuver achieving high slip angles of up to 20° in the front tires, the nonlinear observer tracks the actual slip angle

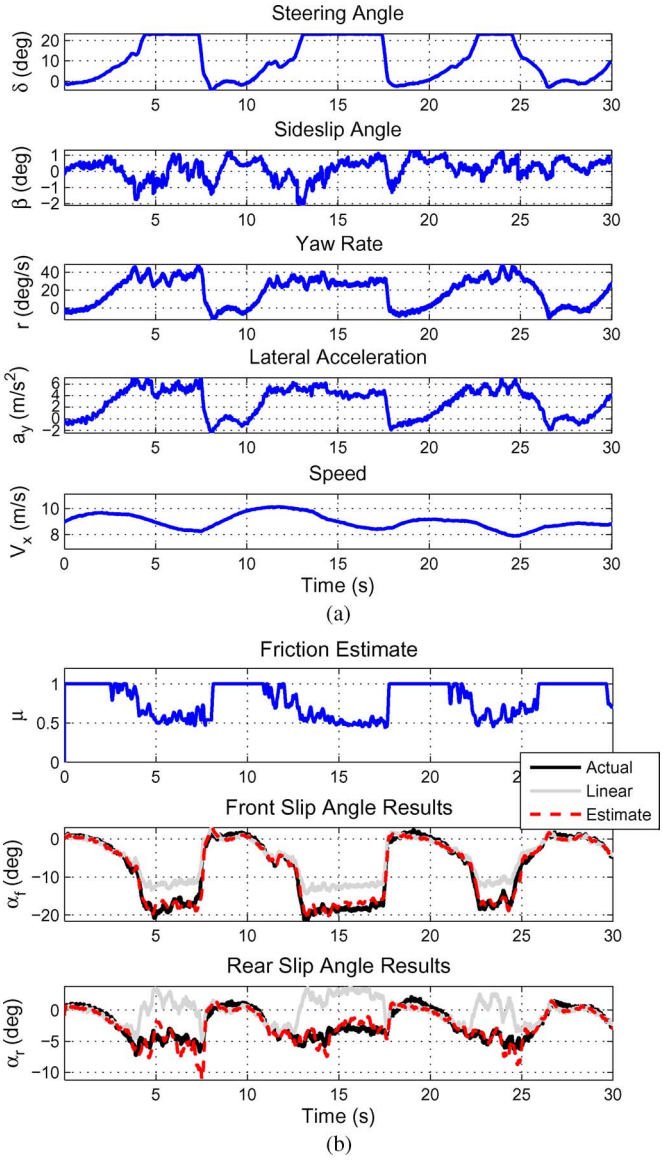

Fig. 12. Experimental transient turns (gravel). (a) Maneuver time history. (b) Estimation results.

much better than the linear estimator. The variation seen in its rear slip angle estimate is likely due to the simple assumptions that available friction on the front and rear axles are equal and that longitudinal weight transfer is negligible. In actuality, the vehicle is traveling over an unevenly distributed gravel surface with changing friction properties. The vehicle also experiences some longitudinal dynamics as the speed undulates during the maneuver. Even so, under these challenging testing conditions, the observer is able to exhibit the robustness of its slip angle and friction estimates.

VII. Conclusion

Tire pneumatic trail is a valuable source of information for lateral tire characterization by enabling early detection of the limits before they are reached. This paper presented an estimation method that utilizes pneumatic trail information contained in steering torque measurements to characterize lateral tire force. Experimental results on two friction surfaces demonstrated that the limits of handling can be predicted once the tires have utilized only 50% of their maximum lateral force. In other words, this method has shown that friction limit detection is possible before the tires have exited the linear handling regime.

Ongoing work is aimed at integrating the estimation method with a stability controller to keep the vehicle operating in a safe handling envelope. The overall observer performance could be improved on P1 with the installation of rear axle load-cell sensors, which would enable direct sensing of the rear tire friction limits. Future work could also incorporate longitudinal tire forces and dynamics in the estimation models to enable accurate estimation when the car is braking or accelerating.

Acknowledgment

The authors would like to thank T. Suzuki, K. Oshiage, D. Yoshitaka, and S. Joe for their support. They would also like to thank R. Hindiyeh, K. Kritayakirana, C. Gadda, and C. Voser for their assistance in this project. The authors would also like to thank the NASA Ames Research Center and the City of Mountain View for allowing access to Moffett Federal Airfield and the Shoreline Lot, respectively, for vehicle testing. Finally, the authors would like to acknowledge the reviewers for their valuable contributions and suggestions.

References

[1] M. Peden, R. Scurfield, D. Sleet, D. Mohan, A. A. Hyder, and E. Jarawan, "World report on road traffic injury prevention," World Health Organization, Geneva, Switzerland, 2004.
[2] Y. Fukada, "Estimation of vehicle slip-angle with combination method of model observer and direct integration," presented at the Int. Symp. Adv. Veh. Control (AVEC), Nagoya, Japan, 1998.
[3] U. Kiencke and A. Daib, "Observation of lateral vehicle dynamics," *Control Eng. Pract.*, vol. 5, no. 8, pp. 1145–1150, 1997.
[4] P. J. T. Venhovens and K. Naab, "Vehicle dynamics estimation using Kalman filters," *Veh. Syst. Dyn.*, vol. 32, pp. 171–184, 1999.
[5] J. Stephant, A. Charara, and D. Meizel, "Virtual sensor: Application to vehicle sideslip angle and transversal forces," *IEEE Trans. Ind. Electron.*, vol. 51, no. 2, pp. 278–289, 2004.
[6] SAE, Warrendale, PA, "Bosch automotive handbook, 6th ed.," 2004.
[7] A. T. van Zanten, "Evolution of electronic control systems for improving the vehicle dynamic behavior," in *Proc. AVEC*, 2002, pp. 7–15.
[8] D. M. Bevly, J. C. Gerdes, C. Wilson, and G. Zhang, "The use of GPS based velocity measurements for improved vehicle state estimation," presented at the Amer. Control Conf. (ACC), Chicago, IL, 2000.
[9] J. Ryu, E. Rossetter, and J. C. Gerdes, "Vehicle sideslip and roll parameter estimation using GPS," in *Proc. AVEC*, 2002, pp. 373–380.
[10] D. M. Bevly, R. Sheridan, and J. C. Gerdes, "Integrating INS sensors with GPS velocity measurements for continuous estimation of vehicle sideslip and tire comering stiffness," presented at the Amer. Control Conf. (ACC), Arlington, VA, 2001.
[11] Y. H. J. Hsu and J. C. Gerdes, "A feel for the road: A method to estimate tire parameters using steering torque," presented at the AVEC, Taipei, Taiwan, 2006.
[12] J.-O. Hahn, R. Rajamani, and L. Alexander, "GPS-based real-time identification of tireroad friction coefficient," *IEEE Trans. Control Syst. Technol.*, vol. 10, no. 3, pp. 331–342, May 2002.
[13] K. Nakajima, M. Kurishige, M. Endo, and T. Kifuku, "A vehicle state detection method based on estimated alignment torque using EPS," SAE, Warrendale, PA, Paper No. 2005-01-1265, 2005.
[14] E. Ono, K. Asano, and K. Koibuchi, "Estimation of tire grip margin using electric power steering system," presented at the 18th Int. Association for Veh. Syst. Dyn. (IAVSD) Symp., Kanagawa, Japan, 2003.
[15] Y. Yasui, W. Tanaka, Y. Muragishi, E. Ono, M. Momiyama, H. Katoh, H. Aizawa, and Y. Imoto, "Estimation of lateral grip margin based on self-aligning torque for vehicle dynamics enhancement," SAE, Warrendale, PA, Paper No. 2004-01-1070, 2004.

[16] M. Endo, K. Ogawa, and M. Kurishige, "Cooperative control of active front steering and electric power steering based on self-aligning torque," presented at the Int. Symp. Adv. Veh. Control (AVEC), Taipei, Taiwan, 2006.
[17] R. Y. Hindiyeh, K. L. R. Talvala, and J. C. Gerdes, "Lanekeeping at the handling limits," presented at the AVEC, Kobe, Japan, 2008.
[18] H. B. Pacejka, "Tire and vehicle dynamics," SAE, Warrendale, PA, 2002.
[19] S. Laws, C. D. Gadda, S. Kohn, P. Yih, J. C. Gerdes, and J. C. Milroy, "Steer-by-wire suspension and steering design for controllability and observability," presented at the IFAC World Congr., Prague, 2005.
[20] Y. H. J. Hsu, S. Laws, C. D. Gadda, and J. C. Gerdes, "A method to estimate the friction coefficient and tire slip angle using steering torque," presented at the ASME Int. Mechan. Eng. Congr. Expo. (IMECE), Chicago, IL, 2006.
[21] H. E. Tseng, "Dynamic estimation of road bank angle," *Veh. Syst. Dyn.*, vol. 36, no. 4–5, pp. 307–328, 2001.
[22] S. Sastry, *Nonlinear Systems: Analysis, Stability, and Control*. New York: Springer-Verlag, 1999.
[23] K. L. Rock, S. A. Beiker, S. Laws, and J. C. Gerdes, "Validating GPS based measurements for vehicle control," presented at the ASME Int. Mechan. Eng. Congr. Expo. (IMECE), Orlando, FL, 2005.

Yung-Hsiang Judy Hsu received the B.S. degree from Harvey Mudd College, Claremont, CA, in 2003, and the M.S. and Ph.D. degrees from Stanford University, Stanford, CA, in 2005 and 2009, respectively.

Her research interests include vehicle dynamics and nonlinear systems control and estimation. Her tire slip angle and peak friction estimation work has a U.S. and Japan Patent Pending JP2005-8062, entitled "Tire State Estimator," submitted in 2008.

Dr. Hsu is an NSF Graduate and Tau Beta Pi Graduate Fellow.

Shad M. Laws received the B.S. degree from Northwestern University, Evanston, IL, in 2003 and the M.S. and Ph.D. degrees from Stanford University, Stanford, CA, in 2005 and 2009, respectively.

His research interests focus on the design, modeling, and control of mechatronic systems, specifically looking at vehicle dynamics and the design of active handling systems. For his dissertation project, he developed an active camber concept for extreme maneuverability—a full-scale prototype with active steer, suspension, and camber to explore tire designs and handling strategies that provide increased cornering ability to the vehicle. Before coming to Stanford, he worked with DSC Environmental, a startup that developed industrial solvent waste recycling systems, and started LN Engineering, a startup that developed and manufactured aftermarket racing engine components.

J. Christian Gerdes received the Ph.D. degree from UC Berkeley, in 1996.

He is an Associate Professor with Stanford University, Stanford, CA, Director of the Stanford Automotive Affiliates Program and Co-Director of the Center for Design Research. His research centers on the application of dynamic modeling to problems in nonlinear control, estimation, and diagnostics. Specific areas of interest include the development of driver assistance systems for lane keeping and collision avoidance, modeling and control of novel combustion processes for Internal Combustion engines and diagnostics for automotive drive-by-wire systems. Prior to joining Stanford, he was the project leader for vehicle dynamics at the Vehicle Systems Technology Center of Daimler-Benz Research and Technology North America. His work at Daimler focused on safety analysis and simulation-based design of heavy trucks for the Freightliner Corporation.